

On the Numerical Modeling of the Thermomechanical Contact for Metal Casting Analysis

Michele Chiumenti
e-mail: michele@cimne.upc.edu

Carlos Agelet de Saracibar
Miguel Cervera

Universidad Politécnic de Cataluña (UPC),
Modulo C1,
Campus Norte, C/Gran Capitán s/n,
08034 Barcelona, Spain

The paper shows the intrinsic difficulties found in the numerical simulation of industrial casting processes using finite element (FE) analysis. Up until now, uncoupled pure thermal simulations have been mostly considered to model solidification and cooling phenomena. However, a fully coupled thermomechanical analysis provides a more complete insight of the casting process and the final outcome regarding the quality of the part. In this type of analysis, the thermomechanical model used plays a role of paramount importance, as the problem is coupled both ways through contact between part and mould. The paper presents the full statement of the problem regarding contact, and it considers the difficulties associated with FE mesh generation and time integration strategy. It also reviews soft and hard algorithms for mechanical contact presenting some new alternatives. Evaluation of coefficients used for thermal contact is also discussed, and a new proposal is presented. Finally, some numerical applications are presented to assess the performance of the proposed strategies both in benchmark and industrial problems.
[DOI: 10.1115/1.2897923]

Keywords: thermomechanical contact, metal casting analysis, heat conduction, heat convection, heat radiation, finite element method

Introduction

The aim of this study is to show the intrinsic difficulties found and the strategy adopted to simulate a *foundry process*.

Up until now, mostly purely thermal simulations have been considered to study the evolution of the solidification and cooling phenomena. This is mainly due to the fact that this strategy is easier and less costly and, therefore, more convenient for large-scale industrial simulations. On the other hand, the *fully coupled thermomechanical analysis* is the natural framework to represent the heat flow exchange, the final shape of the casting part, as well as the evolution of the residual stresses induced by the manufacturing operations. The accurate modeling of both stresses and deformations of the part during the solidification and the cooling phases is crucial to capture the thermal pattern (temperature and solidification evolution) in aluminum casting or, more generally, when a permanent mould is used. In fact, the thermal deformation of both part and mould modifies the original interfacial heat transfer among all the casting tools involved in the process. The relationship between the heat transfer coefficient and mechanical quantities such as the open air gap or the contact pressure has been experimentally proved. Hence, the mechanical analysis coupled with the thermal simulation is mandatory to produce a reliable casting numerical model.

More specifically, this work will focus on the description of the *thermomechanical contact model* necessary to study the interaction among all the casting tools during the solidification and cooling processes. This is possibly the key point in a casting simulation, playing an extremely important role and coupling the thermomechanical problem in both ways.

Governing Equations

The system of partial differential equations governing the coupled thermomechanical problem is defined by the momentum

and energy balance equations, restricted by the inequalities arising from the second law of thermodynamics. This system must be supplemented by suitable constitutive equations and prescribed boundary and initial conditions.

Strong Form of the Governing Equations. Using a mixed \mathbf{u}/p displacement/pressure formulation, the strong forms of the momentum and energy balance equations are given by

$$\nabla \cdot \mathbf{s} + \nabla p + \mathbf{b} = \mathbf{0} \quad (1)$$

$$\dot{E} = \boldsymbol{\sigma} : \dot{\boldsymbol{\epsilon}} + \dot{Q} \quad (2)$$

where \mathbf{s} is the deviatoric part of Cauchy's stress tensor defined as $\boldsymbol{\sigma} = p\mathbf{1} + \mathbf{s}$, \mathbf{b} is the vector of forces per unit of volume, \dot{E} is the rate of the internal energy per unit of volume, and $\dot{Q} = \dot{R} - \nabla \cdot \mathbf{Q}$ is the heat supplied to the system per unit of volume due to the internal sources per unit of volume \dot{R} and input heat flow through the boundary $-\nabla \cdot \mathbf{Q}$.

On the other hand, the second law of thermodynamics limits the direction of the energy transformations and it postulates that there exists a state function called enthalpy H so that $\dot{H} = \dot{Q} + \dot{D}$, where $\dot{D} \geq 0$ is the thermomechanical dissipation and it represents the energy dissipated (transformed in heat) for an irreversible process.

Weak Form of the Balance of Momentum Equation. Let $\delta \boldsymbol{\eta}$ and δq be the test functions associated with the displacement and pressure fields \mathbf{u} and p , respectively. The weak form of the balance of momentum equation in the hypothesis of a quasistatic process can be expressed in the mixed format as

$$\begin{aligned} & \int_{\Omega} (\nabla^S \delta \boldsymbol{\eta} \boldsymbol{\eta}) dV + \int_{\Omega} (\nabla \cdot \delta \boldsymbol{\eta} p) dV \\ & = \int_{\Omega} (\delta \boldsymbol{\eta} \mathbf{b}) dV + \int_{\partial \Omega} (\delta \boldsymbol{\eta} \bar{\mathbf{t}}) dS + \int_{\partial \Omega} (\delta \boldsymbol{\eta} \mathbf{t}_c) dS \end{aligned}$$

Contributed by the Heat Transfer Division of ASME for publication in the JOURNAL OF HEAT TRANSFER. Manuscript received February 6, 2007; final manuscript received January 25, 2008; published online April 23, 2008. Review conducted by Ben Q. Li.

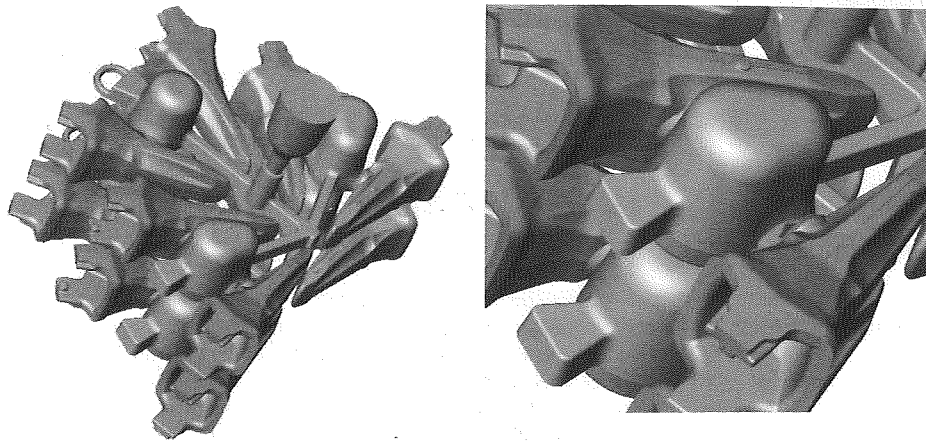


Fig. 1 Sand gravity casting; CAD geometry of the foundry system

$$\int_{\Omega} \delta q \left(\nabla \cdot \mathbf{u} + \frac{p}{K} - e^{\theta} \right) dV = 0 \quad (3)$$

where K is the bulk modulus, e^{θ} is the thermal (volumetric) deformation, and $\bar{\mathbf{t}}$ and \mathbf{t}_c are the prescribed and contact tractions, respectively. Observe that for a liquidlike behavior, $K \rightarrow \infty$ and $e^{\theta} = 0$, the second equation reads

$$\int_{\Omega} (\delta q \nabla \cdot \mathbf{u}) dV = 0 \quad (4)$$

stating (in weak form) the incompressibility condition $\nabla \cdot \mathbf{u} = 0$. Hence, a stabilization technique becomes necessary to ensure stability. It can be proved that neither standard P1 nor P1/P1 mixed elements pass the Babuska–Brezzi stability condition [1]. An attractive alternative to circumvent such condition can be achieved introducing a stabilizing term in the continuity equation. A first possibility is the so called Galerkin least-squares (GLS) method, which introduces an element-by-element stabilization term based on the residual of the momentum balance equation or as an attractive alternative the *orthogonal subgrid scale* (OSGS) approach [2–6].

Weak Form of the Balance of Energy Equation. Let $\delta\vartheta$ be the test function associated with the temperature field T . The weak form of the balance of energy equation reads

$$\int_{\Omega} (\delta\vartheta \dot{H}) dV + \int_{\Omega} [\nabla(\delta\vartheta) k \nabla T] dV = \int_{\partial\Omega} (\delta\vartheta Q_c) dS \quad (5)$$

where Fourier's law has been introduced as $\mathbf{Q} = -k \nabla T$, being k the conductivity coefficient. Observe that for casting application the dissipation term \dot{D} is negligible and usually does not exist neither as the source term \dot{R} nor any prescribed heat flux at the boundary. The only driving force that moves the problem is Q_c , which is the heat flux at the boundary interfaces due to the thermal contact interaction.

This term is possibly the most important one for this kind of applications and, as it will be shown in the next sections, it is responsible for the coupling between the mechanical and the thermal problems. On one hand, all the mechanical properties, that is, the material behavior, depend on the temperature field; on the other hand, it will be shown that the heat flux at the contact interfaces Q_c depends on mechanical quantities such as the normal contact pressure or the thermal shrinkage of all the foundry components.

Given this, it is not possible to uncouple the problem so that both thermal and mechanical solutions must be obtained at each

time step. In this work, the authors chose a staggered solution strategy based on the fractional step method. Interested readers can refer to Refs. [7,8] for further details.

Geometry and FE Mesh

Once the equations to be solved are defined, the main difficulty to be taken into account when modeling a casting process is the geometrical definition of all the casting tools involved in the manufacturing process. The complexity of such geometries makes the meshing operation really difficult. Figure 1 shows the intricacy of the sand casting system used to manufacture excavator teeth.

The high number of casting tools involved in the simulation such as part, molds, cores, cooling channels, chillers, etc., requires an important computer-aided design (CAD) effort, which turns into much greater meshing troubles.

Generally, only a tetrahedral finite element (FE) mesh can be generated. The small thickness of many parts, especially in the case of either low-pressure or high-pressure die-casting processes, is a strong constraint when meshing. Very few elements are placed within the thickness of the casting part, posing difficulties for the numerical description of temperature gradients as well as the evolution of the thermal contraction or the stress field.

The artificial stiffening due to a very coarse mesh discretization is possibly the major difficulty to achieve the result accuracy needed. Figure 2 shows the original CAD geometry and the FE mesh used for a high pressure die-casting (HPDC) analysis. The mesh generated, including mould and filling system, is about 1×10^6 of linear elements, which is the current practical limit in a standard personal computer (PC) platform. However, just one linear element is placed through the thickness of the part.

The artificial stiffening of the discrete model induced by a coarse mesh is increased by the element technology used to respect the volumetric incompressibility constraints as introduced in the previous section. Mechanical contact algorithms particularly suffer such numerical stiffening and, therefore, a very robust contact algorithm must be used to prevent spurious penetrations and numerical locking of the solution.

The discretization of the contact surface is another problem induced by the FE mesh. Surface curvature results in a nonsmooth surface definition, leading to a nonsmooth contact reaction field. The direction of the normal vector at each node of the surface is not univocally defined: There are different possibilities according to the algorithm selected. All these possibilities should converge refining the mesh but if this is not possible (i.e., a large industrial analysis), the choice can seriously affect the final result.

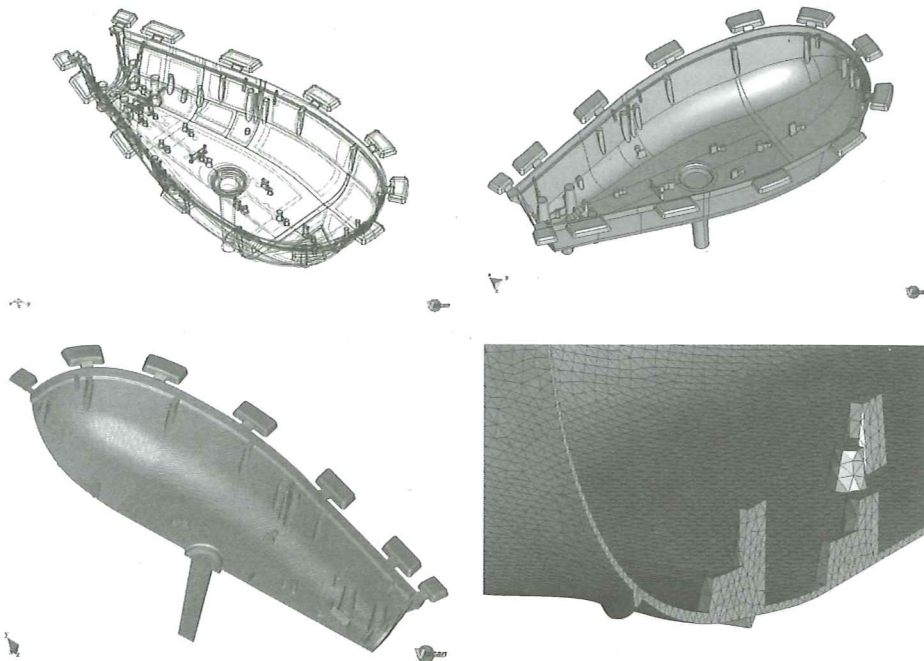


Fig. 2 HP die-casting process: CAD geometry and FE mesh generated

Thermomechanical Contact Algorithms

On foundry processes, the numerical simulation of the mechanical interaction among casting tools such as part, mould, cores, etc., is an extremely important issue to be taken into account. Looking at the definition of heat conduction and heat convection laws, it is clear how important is an accurate definition of the contact pressure as well as the prediction of the open air gaps between casting part and mould surfaces. The relationship between heat transfer coefficients and open air gap has been experimentally proved [9,10], especially in the case of low-pressure as well as HPDC processes, which use permanent moulds.

In the literature, it is possible to find many different algorithms to study the mechanical contact between deformable bodies [11,12]. In a solidification process, the shrinkage of the casting material is of order of 3–5% of the original volume and no other movements are allowed, so that it is possible to assume a small displacement contact algorithm. This hypothesis reduces the cost associated with the so called *closest-point-projection* procedure, which is commonly used when large slips can occur [13]. A simpler node-to-node or face-to-face contact algorithm can be assumed without loss of accuracy. Therefore, coincident surface meshes are generated such that the location of the boundary nodes of the mould matches the location of the casting nodes. Observe, as great advantage of such strategy, that neither spurious initial penetrations nor fictitious open gaps are allowed at the beginning of the simulation.

Once the contact zone is identified and discretized, two different typologies of contact algorithms can be applied to prevent the penetration establishing the contact constraints. On one hand, the so called *soft contact* algorithms are based on penalization techniques, such as the *penalty* method or the *augmented Lagrangian* algorithm, among others [14,15,13]. On the other hand, the so called *hard contact* algorithms based on the computation of the contact reactions totally prevent the penetration at the contact interface, such as the *Lagrange multiplier* method [11].

In a penalty approach, the final penetration is not zero and it depends on the value of the penalty parameter selected. This is a major problem in the case of casting analysis because it is really difficult to select the appropriate penalty value. In practice, this value is usually taken as a function of the stiffness and element

sizes of the contacting bodies. It is also a fact that during both the solidification and the cooling processes, casting stiffness drastically changes, leading to a hard choice of the penalty. Some authors propose a temperature dependent parameter according to the temperature evolution at the casting interface [16,17]. Even if the results achieved are better, the use of fairly large values of the penalty parameter to prevent the penetration of one boundary through the other is still problematic.

It must also be observed that the use of iterative solvers, such as a conjugate gradient or GMRES iterative solvers, is a really attractive alternative for the solution of large-scale industrial problems. The number of iterations necessary to achieve the solution is a function of the condition number of the matrix of the system. By adding the contact contributions to the assembled matrix (which depend on the value of the penalty parameter used), the number of iterations required by the solver to converge increases, and as a direct consequence, the total CPU time. High values of the penalty parameter lead to a matrix ill conditioning up to the limit case of solver locking.

A possibility to reduce the matrix ill conditioning, without losing result quality, is the augmented Lagrangian method [14]. The drawback is the terrible CPU time increase.

As a third possibility, proposed here by the authors, a block-iterative solution can be considered. The basic idea consists of using a penalty method together with the decomposition of the final system of equations into casting, mold, and contact equations, such as

$$\begin{bmatrix} \mathbf{A}_{\text{cast}} & \mathbf{0} & \mathbf{A}_{c,\text{cast}} \\ \mathbf{0} & \mathbf{A}_{\text{mold}} & \mathbf{A}_{c,\text{mold}} \\ \mathbf{A}_{c,\text{cast}} & \mathbf{A}_{c,\text{mold}} & \mathbf{A}_c \end{bmatrix} \begin{Bmatrix} d\mathbf{u}_{\text{cast}} \\ d\mathbf{u}_{\text{mold}} \\ d\mathbf{u}_c \end{Bmatrix} = \begin{Bmatrix} \mathbf{r}_{\text{cast}} \\ \mathbf{r}_{\text{mold}} \\ \mathbf{r}_c \end{Bmatrix} \quad (6)$$

where the contact equations are those associated with the nodes at the contact interface. As a result, an arrow shaped system of equations is obtained. An iterative solution of such a system is proposed in the form

$$\mathbf{A}_{\text{cast}} d\mathbf{u}_{\text{cast}}^{i+1} = \mathbf{r}_{\text{cast}} - \mathbf{A}_{c,\text{cast}} d\mathbf{u}_c^i$$

$$\mathbf{A}_{\text{mold}} d\mathbf{u}_{\text{mold}}^{i+1} = \mathbf{r}_{\text{mold}} - \mathbf{A}_{c,\text{mold}} d\mathbf{u}_c^i$$

Table 1 Typical convergence performance obtained using the standard penalty method, the augmented Lagrangian algorithm, and the proposed block-iterative method

Penalty method	Convergence ratio	Augmented Lagrangian	Convergence ratio	Block-iterative method	Convergence ratio
Iter=1	1.000000E+3	Iter=1	1.000000E+3	Iter=1	1.000000E+3
Iter=2	2.245836E+2	Iter=2	8.957635E+2	Iter=2	6.84654E+1
Iter=3	2.093789E+2	Iter=3	7.846474E+0	Iter=3	8.57626E-2
Iter=4	7.473996E+1	Iter=4	6.735237E-3	Block-iter	
Iter=5	5.873453E+1	New augm		Iter=4	2.97468E+1
Iter=6	9.986438E+0	Iter=5	5.734238E+1	Iter=5	4.845342E-2
Iter=7	3.762686E-2	Iter=6	6.723579E-3	Block-iter	
Iter=8	2.125986E-4	New augm		Iter=6	4.734127E-3
		Iter=7	3.946447E-3		

$$A_c du_c^{i+1} = r_c - A_{c,cast} du_{cast}^{i+1} - A_{c,mold} du_{mold}^{i+1} \quad (7)$$

where index (*i*) stands for the iteration counter within the block-iterative solution.

The advantages of such procedure are manifold. First, the local matrices that solve each of the subproblems generated are much better conditioned, leading to a much better performance of any iterative solver chosen. Second, the partial problems to be solved are smaller and consequently faster to solve and, finally, the proposed structure can be easily parallelized so that casting and mold can be assembled and solved using different processors. Observe that the only information to be transferred is the vector of nodal unknowns. As a drawback of the method, it must be pointed out that the number of iterations required by the block-iterative method proposed depends on the penalty parameter used. Therefore, even if a better control on the global solution is achieved, the performance still depends on the conditioning of the original matrix.

In Table 1, it is possible to observe the typical Newton-Raphson convergence evolution for the three methods described. The augmented Lagrangian method shows a faster convergence evolution if compared to the standard penalty algorithm. On the other hand, the total number of iterations necessary to solve the time step is higher, leading to a longer CPU time. Looking at the block-iterative method, it is possible to judge the good performance of the Newton-Raphson convergence even if the total number of iterations is still high.

Note that the block-iterative procedure gives a solution even if the iterative loop is not fully converged, allowing the solution of the following time step without stopping the full simulation process due to a loss of convergence of the global analysis.

Thermal Contact Model

Accurate knowledge of the interfacial heat transfer coefficient between the solidifying casting and the surrounding mould is essential to produce a realistic solidification model. Hence, a reliable thermal contact model must be considered taking into account the heat transfer when the surfaces are in contact or when it exists as an open air gap [16].

Closed-Gap Thermal Contact Model. We refer to *closed-gap* thermal contact model Q_{closed} when the casting surface is in contact with the mould surface. In such case, standard Fourier's law cannot describe the heat transfer phenomena because the contacting surfaces do not physically match perfectly, leading to different temperatures at the casting and the mould surfaces (see Fig. 3). A heat resistance due to the gas trapped among the surface asperities can be experimentally observed. This resistance reduces as the contact pressure increases because the *effective* contact area extends.

The heat flux is computed as the product of a heat transfer coefficient, h_{closed} , multiplied by the thermal gap, $g_{\theta} = T_{cast} - T_{mould}$, existing between the casting and mould surfaces in the form

$$Q_{closed} = h_{closed}(t_n)(T_{cast} - T_{mould}) \quad (8)$$

It must be observed that the h_{closed} is the inverse of the heat resistance coefficient, meaning that high values of the h_{closed} result into small values of the heat resistance. As a limit, an infinite value of the h_{closed} means that there is no heat resistance and Fourier's law governs the heat flux between the two bodies.

As it was commented above, the heat transfer coefficient can be

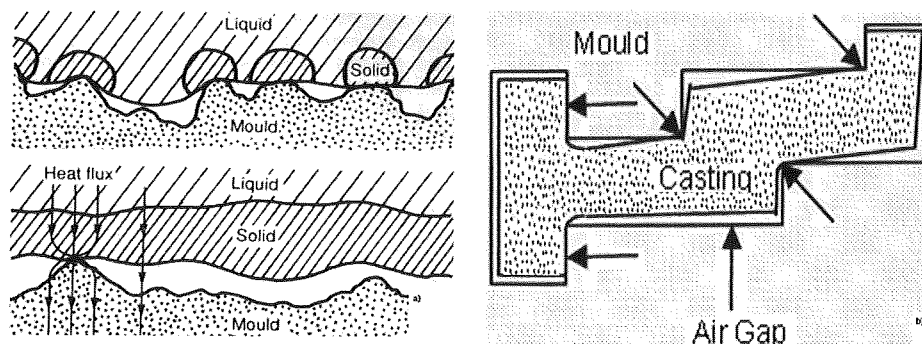


Fig. 3 Thermal contact model. (a) The heat conduction coefficient is a function of the effective contact area, which depends on the contact pressure. (b) Depending on the casting shrinkage, thermal conduction or thermal convection must be considered.

assumed as a function of the normal contact pressure, t_n , between the two contacting surfaces. The model proposed computes a thermal resistance, R_{closed} , due to the air trapped in between the mould and the casting surfaces and induced by the roughness values measured on those surfaces. In addition, the thermal resistance due to the mould coating is also accounted so that the total thermal resistance can be expressed by

$$R_{\text{closed}} = \frac{R_z}{k_{\text{air}}} + \frac{\delta_{\text{coat}}}{k_{\text{coat}}} \quad (9)$$

where $R_z = 0.5\sqrt{R_{z,\text{cast}}^2 + R_{z,\text{mould}}^2}$ is the mean peak-to-valley height of the rough surfaces, δ_{coat} is the effective thickness of the coating, and k_{air} and k_{coat} are the thermal conductivities of the gas trapped and the coating, respectively.

The effect induced by contact pressure is modeled according to the experimental evidence using the following expression:

$$h_{\text{closed}}(t_n) = \frac{1}{R_{\text{closed}}} \left(\frac{t_n}{H_e} \right)^b \quad (10)$$

where H_e is the Vickers hardness and $0.6 \leq b \leq 1.0$ is a constant exponent [9,10]. Observe that the model assumes a h_{close} proportional to the normal contact pressure as a measure for the effective contact surface interaction.

Open-Gap Thermal Contact Model. Heat convection between two bodies appears when they separate one from the other due to the thermal shrinkage effect. The model considered by the authors does not pretend to describe the air convection between the two surfaces: The surrounding air is neither discretized nor studied. The model only looks for the effects on the heat transfer between the two bodies. An *open-gap* heat flux Q_{open} is assumed to describe this phenomenon following the so called *Newton law of cooling*. Such heat flux is defined as a function of a coefficient, h_{open} , multiplied by the thermal gap in the form

$$Q_{\text{open}} = h_{\text{open}}(g_n)(T_{\text{cast}} - T_{\text{mould}}) \quad (11)$$

It can be verified experimentally that the heat transfer coefficient, h_{open} , depends on the open air gap, g_n (the distance between the two surfaces) due to the insulating effect of the gas trapped in the cavity:

$$h_{\text{open}}(g_n) = \frac{k_{\text{air}}}{g_n} \quad (12)$$

On the other hand, it must be observed that the above expression must be limited with the value assumed by the heat transfer coefficient when the gap is close so that

$$h_{\text{open}} = \min\left(\frac{k_{\text{air}}}{g_n}, h_{\text{close}}\right) \quad (13)$$

The model presented above is recommended for permanent mould casting. This is the case of low-pressure and HPDC technologies. The high conductivity of the metallic (steel) mould drops down when an air gap is formed due to the shrinkage of the casting material. Air (trapped gas) conductivity is much lower than the steel conductivity and the insulating effect is evident.

Observe that either the contact pressure (used to compute the heat conduction coefficient) or the gap formation can be taken into account only if a *coupled thermo mechanical simulation* is performed. Both solidification and cooling evolution are driven by the heat flux exchanged through the boundaries and such heat flux is coupled with the mechanical behavior. If a purely thermal model is used to compute the solidification evolution, a lack of information must be assumed and a simplified model for the heat flux exchange must be considered.

In this case, both open-gap and closed-gap heat fluxes can only depend on the temperature field, which is the only nodal variable computed. Both models reduce to

$$Q_{\text{ther}} = h_{\text{ther}}(T_{\text{cast}} - T_{\text{mould}}) \quad (14)$$

where the heat transfer coefficient, h_{ther} , can be only a function of the temperature field. Proposals introduced by different authors assume as driving variables the temperature of the casting surface, or the temperature of the mould surface, or even an average (air) temperature field.

In our opinion, the temperature field at the contact surface is not representative of the heat flux behavior and it is not possible to distinguish between open-gap and closed-gap heat behaviors because the mechanical gap is not computed. It is easy to observe, experimentally as well as numerically, that the surface temperature of the casting material drops very rapidly when coming in contact with the mould. The surface skin becomes solid even if the casting volume is still mainly liquid. As a consequence, the temperature field on the surface is not representative of the solidification evolution of the part (thermal shrinkage).

To overcome this problem, we propose a heat transfer coefficient as a function of the percentage of solidified casting material, $h_{\text{ther}}(F_S)$, where F_S takes into account the evolution of the solidification as

$$F_S = \frac{1}{V} \int f_S(T) dV \quad (15)$$

where $0 \leq f_S(T) \leq 1$ is the solid fraction function computed at each point of the casting volume. As a result, the heat flux is defined as a function of the volumetric contraction of the casting that is an average open air gap all around the part. Given this, the heat transfer coefficient is computed as

$$h_{\text{ther}}(F_S) = F_S \bar{h}_{\text{open}} + (1 - F_S) \bar{h}_{\text{close}} \quad (16)$$

where \bar{h}_{close} and \bar{h}_{open} are average values for the heat conduction and heat convection coefficients, respectively.

Heat Convection Model: The Newton Law of Cooling. Observe that a heat convection model should be considered to study the cooling of the casted part induced by the surrounding environment during the demolding operation. Also, in this case, the FE discretization only studies the thermomechanical behavior of the bodies without considering the air. The proposed model is based on the Newton law of cooling considering the heat flux as the product between a heat transfer coefficient and the thermal gap:

$$Q_{\text{conv,env}} = h_{\text{env}}(T_{\text{env}})(T_{\text{mould}} - T_{\text{env}}) \quad (17)$$

Note that the heat transfer coefficient depends on the casting temperature in contact with the environment $h_{\text{env}}(T_{\text{cast}})$, assuming that the air convection generated is proportional to the existing thermal gap.

Heat Radiation Model. Heat radiation flux between two facing bodies is computed using the Stefan-Boltzmann law:

$$Q_{\text{rad}} = h_{\text{rad}}[(T_{\text{cast}} + 273.16)^4 - (T_{\text{mould}} + 273.16)^4] \quad (18)$$

where the heat radiation coefficient h_{rad} depends on the emissivities of the two bodies, ϵ_{coat} and ϵ_{mould} , respectively, and Stefan's constant σ_a as

$$h_{\text{rad}} = \frac{\sigma_a}{(1/\epsilon_c + 1/\epsilon_m - 1)} \quad (19)$$

It must be pointed out that, for casting analysis, the two surfaces are coincident so that the view factors can be neglected.

Finally, when the heat is dissipated through the surrounding environment during demolding, the radiation law is expressed in the form

$$Q_{\text{rad,env}} = \sigma_a \epsilon_{\text{cast}}[(T_{\text{cast}} + 273.16)^4 - (T_{\text{env}} + 273.16)^4] \quad (20)$$

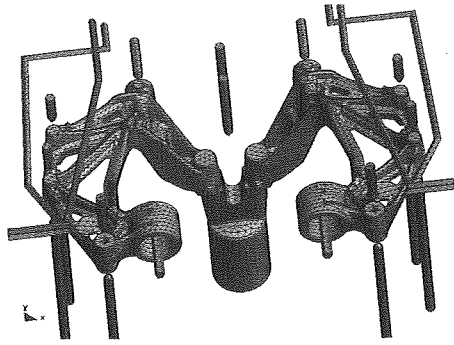


Fig. 4 Automotive part; FE mesh generated for the casting and the cooling system

Numerical Simulations

The formulation presented in previous sections is illustrated here with a number of numerical simulations. The goal is to demonstrate the good performance of the proposed formulation in the framework of infinitesimal strain coupled thermal plasticity for industrial casting analyses and, in particular, for steel mould casting. Computations are performed with the FE code VULCAN developed by the authors at the International Center for Numerical Method in Engineering (CIMNE) in Barcelona, Spain, and commercialized by QUANTECH-ATZ [18]. In all the simulations, the Newton-Raphson method, combined with a line-search optimiza-

tion procedure, is used to solve the nonlinear system of equations arising from the spatial and temporal discretizations of the weak form of the governing equations. Convergence of the incremental iterative solution procedure was monitored by requiring a tolerance of 0.1% in the residual based error norm.

Penalty Versus Augmented Lagrangian Method. This example is intended to show the important role played by the element size. It is easy to understand that the finer the mesh used is, the more deformable is the body defined in the FE mesh, allowing the use of lower values of the penalty parameter to achieve a good solution. Figures 5(a) and 5(b) show two different mesh discretizations used to demonstrate the performance of the soft contact formulation. The contact benchmark consists of the upsetting of the upper block pressed against the base block. To increase the difficulty, the material stiffness of the base block is ten times higher compared to the other block.

This benchmark tries to reproduce the situation that one should face when solving a real industrial solidification analysis. Figure 4 shows an automotive casting part and the corresponding FE mesh. Half a million elements are necessary to mesh the full casting system including cooling channels and mould. Even if the mesh looks good and the total number of elements is close to the computational limit in a standard PC, few elements are placed in the thickness of the part. Hence, mechanical contact presents the same problem shown by the coarse mesh in the contact benchmark.

Figures 6(a) and 7(a) show the convergence of both the contact reaction and the contact penetration when the penalty parameter is increased. Figure 6(b) shows what happens when the coarse mesh is used. It is not possible to achieve the converged solution for

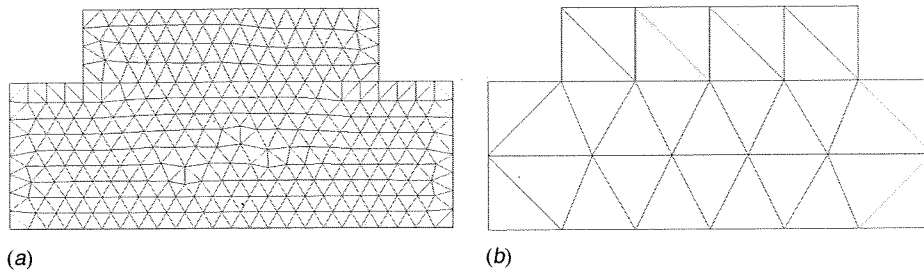


Fig. 5 Contact benchmark: (a) fine mesh and (b) coarse mesh

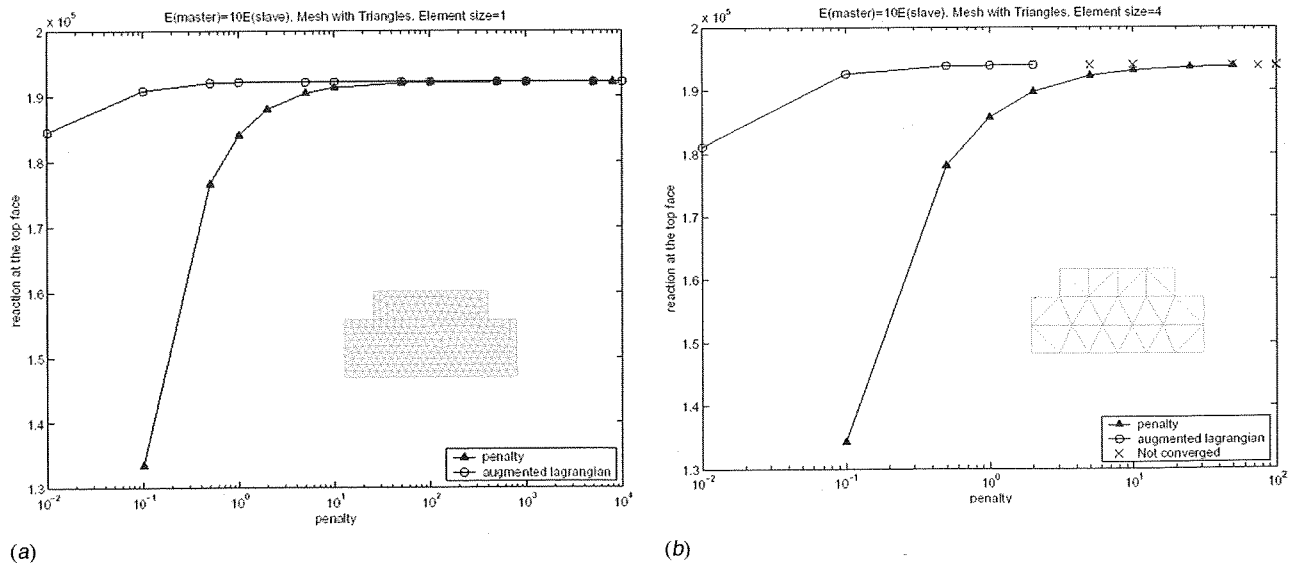
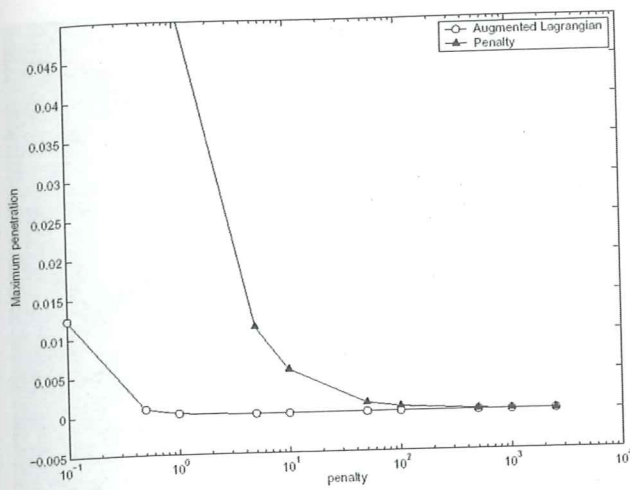
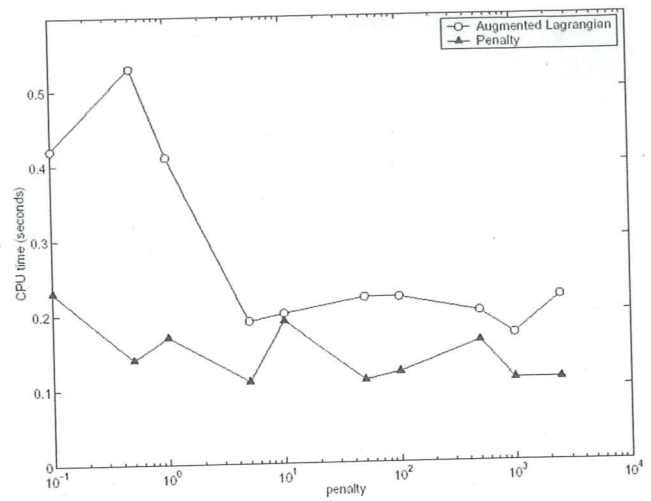


Fig. 6 Contact reaction for both the penalty and the augmented Lagrangian methods when increasing the penalty parameter: (a) fine mesh and (b) coarse mesh



(a)



(b)

Fig. 7 Contact benchmark comparison between penalty and the augmented Lagrangian methods: (a) convergence of the contact penetration to satisfy contact impenetrability constraint when increasing the penalty parameter and (b) CPU time

high values of the penalty parameter due to locking of the analysis. The convergence to the final solution is slower and often it cannot be achieved. In fact, locking of the solution is the main drawback of the penalized methods. Roughly speaking, if a penetration is detected, then a contact element is generated. The stiffness of such element in the direction normal to the surface is set to a very high value compared to the material stiffness of the contacting bodies. Observe that, to get zero penetration and fully satisfy the impenetrability constraint imposed by the contact condition, an infinite value should be given to the penalty parameter. This is not possible and it can be demonstrated that the maximum value that can be used corresponds to the maximum eigenvalue of the final system of equations to be solved. In many occasions, this value is not large enough to prevent penetration and if one tries to increase it, then locking of the solution occurs.

The augmented Lagrangian algorithm is possibly the most used solution to overcome this problem, enabling the use of lower values for the original penalty parameter. It can be observed in Figs. 6(a) and 7(a) how the augmented Lagrangian method has a better performance to achieve the converged solution using lower values for the penalty parameter. On the other hand, Fig. 7(b) clearly presents the weakness of the method in terms of CPU time. Augmented Lagrangian is two or three times slower than the standard penalty method. Hence, even if the choice of a correct penalty

parameter is less problematic, the CPU time increases significantly. According to the experience of the authors, this method is not efficient for large-scale computations.

Thermomechanical Solidification Benchmark. This example is concerned with the solidification process of a cylindrical aluminum specimen in a steel mould. The main goal of this benchmark is to show the accuracy of the full coupled thermomechanical contact model proposed for a solidification analysis. The numerical results have been compared to the experimental values in Ref. [19]. The experiment consists of the solidification of commercially pure aluminum into an instrumented mould. Thermocouples have been placed in the mould wall and in the mould cavity. The thermocouple locations are shown in Fig. 8. Two quartz rods were inserted into the mould to measure both the displacement of the solidifying cylinder and the mould expansion. The geometry of the problem is shown in Fig. 8. The starting conditions assumed for the numerical simulation consider a completely filled mould with aluminum in the liquid state at a uniform temperature of 670°C, and an initial temperature of the mould was set to 200°C. A thermoelastic constitutive model has been used to simulate the material behavior of both the aluminum casting and the steel mould. The external surfaces of the mould as well as the upper surface of the casting metal have been assumed perfectly insu-

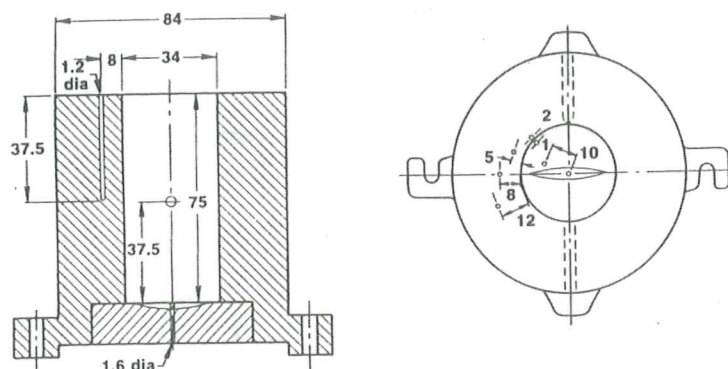


Fig. 8 Cylindrical aluminum solidification test; geometry of the experimental apparatus and location of both thermocouple and displacement transducers

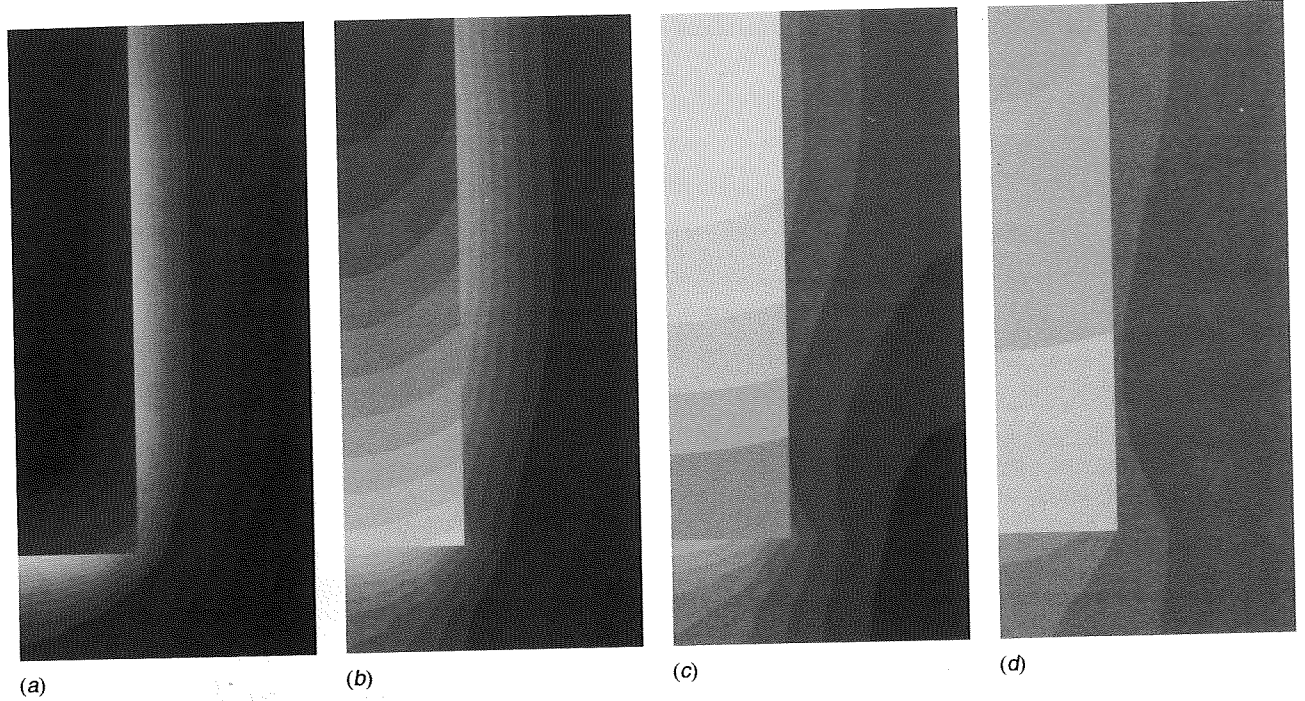


Fig. 9 Cylindrical aluminum solidification test; temperature evolution: (a) 10 s, (b) 20 s, (c) 40 s, and (d) 90 s

lated. A constant heat transfer coefficient by conduction $h_{\text{cond}} = 2300 \text{ W/m}^2\text{s}$ has been assumed as the limit value of the convection-radiation heat flux existing between the aluminum part

and the steel mould as a function of the open air gap (Fig. 9). Figure 10 shows the temperature evolution at the casting center, casting surface, and mould surface compared to the experimental

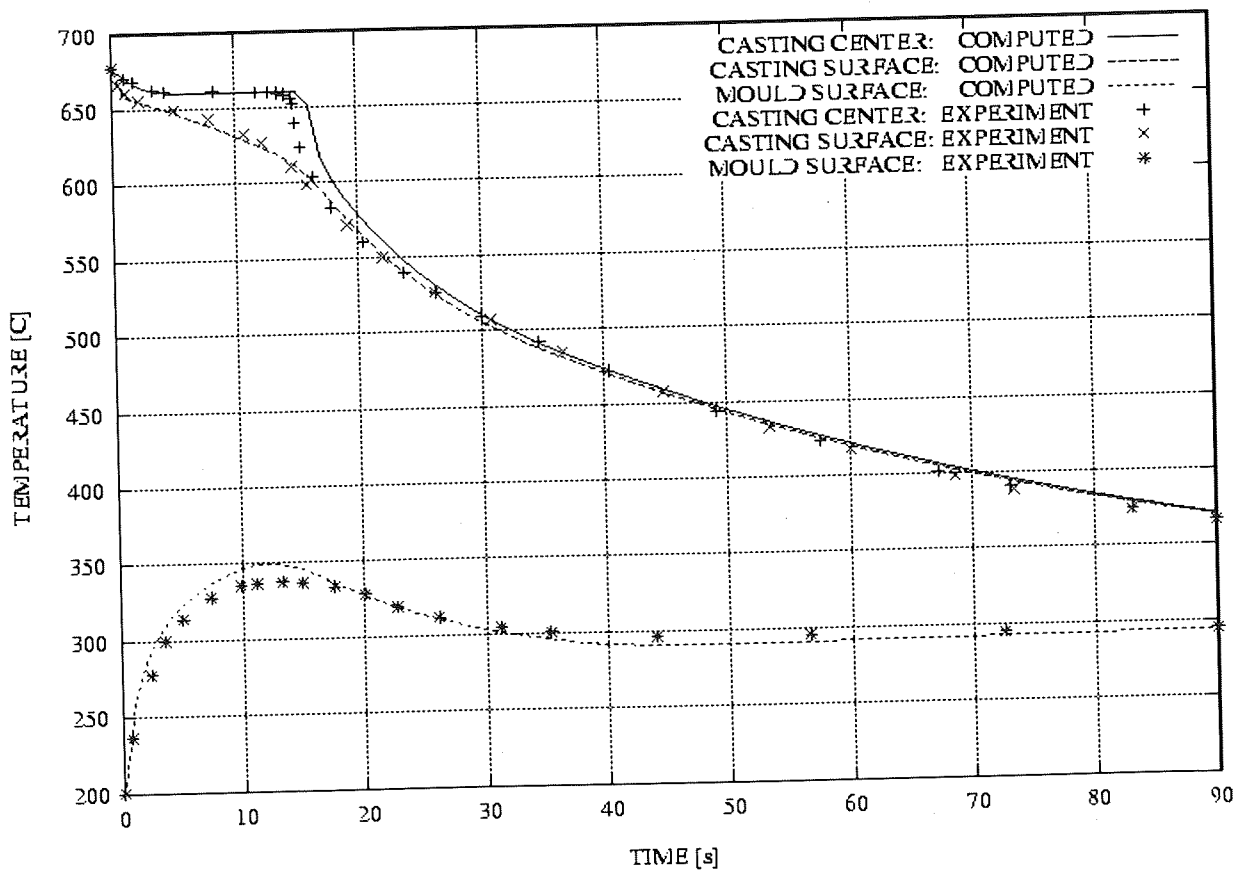


Fig. 10 Comparison between computed and experimental values of the temperature at the casting center, casting surface, and mould surface, respectively

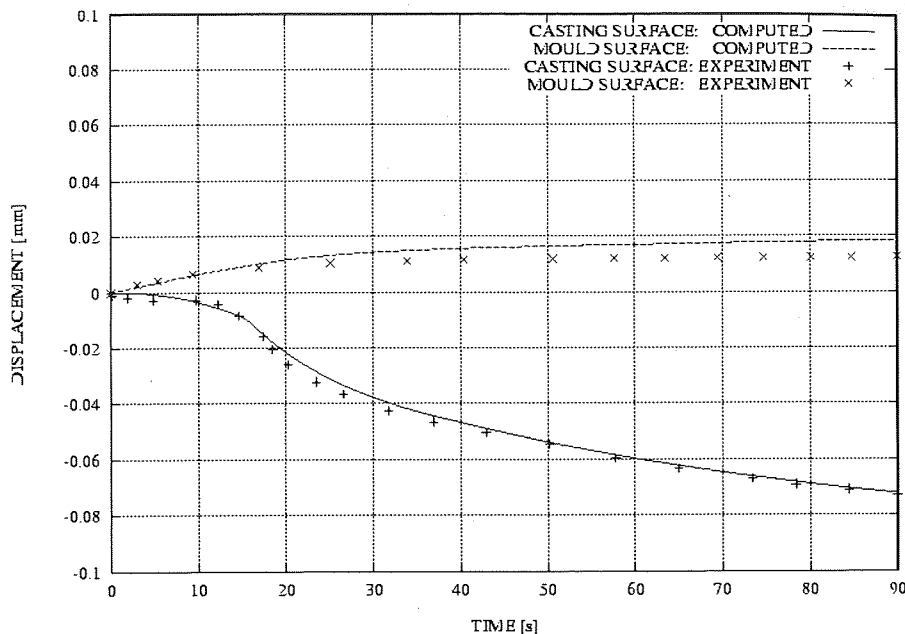


Fig. 11 Comparison between computed and experimental values of the radial displacement on the casting surface and mould surface, respectively

data. Figure 11 shows the evolution of the radial displacements for both casting and mould surfaces. The difference between the two curves corresponds to the evolution of the open air gap. Temperature and air gap evolutions predicted by the model compare very well with the experimental results demonstrating the accuracy of the thermomechanical model presented [20,21].

Foundry Simulation of an Aluminum Motor Block. The final numerical simulation is concerned with the solidification process of an aluminum motor block in a steel mould. Geometrical and material data were provided by the TEKSID Aluminum Foundry Division. The full mesh, including the mould, consists of 580,000 tetrahedral elements. The aluminum material behavior has been modeled by the fully coupled thermoviscoplastic model, while the steel mould behavior has been modeled by a simpler thermoelastic model. The initial temperature is 700°C for the casting and is 300°C for the mould. The cooling system has been kept at 20°C. The temperature evolution as well as thermal shrinkage during solidification are shown in Fig. 12. Figure 13 shows the temperature, von Mises deviatoric stresses, and equivalent plastic strain distributions.

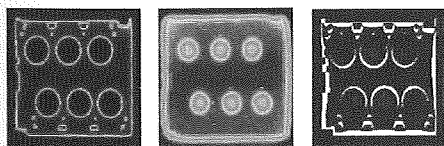


Fig. 12 Temperature and shrinkage evolution (plane xy)

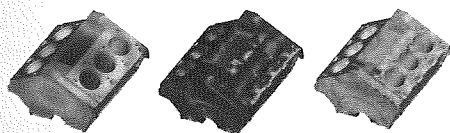


Fig. 13 (a) Temperature, (b) J2 von Mises, and (c) plastic strain distributions

Concluding Remarks

In a foundry analysis, many casting tools must be represented. Nowadays, the mesh discretization that can be adopted for the computation in a standard PC is, unfortunately, generally too coarse. Very few elements can be placed in the thickness of the casting, especially if HPDC processes must be simulated. The low capability to capture the high temperature gradients, the solidification process, as well as the contact interaction makes an accurate simulation difficult to achieve. Moreover, the complexity of the CAD geometry obliges the use of tetrahedral elements inducing high numerical stiffening in the solution. This problem is augmented when the incompressibility constraint is enforced as in the case of liquidlike behavior or J2-plasticity constitutive law.

The nonsmooth description of the contacting surfaces is another consequence introduced by the mesh discretization: The normal vector to the surface is nonunivocally defined and in the case of coarse meshes, the contact reaction field is not uniformly spread.

Furthermore, the use of large time steps as well as the loss of constraint induced by the shrinkage effect of the casting make the analysis highly nonlinear.

The thermomechanical contact plays an extremely important role in a casting analysis, driving the solidification and the following cooling phase. A novel definition of the heat transfer coefficient for purely thermal analysis has been proposed. On the other hand, the dependency on mechanical quantities such as the contact pressure or the open air gap makes the difference when selecting the contact algorithm to correctly represent the mechanical constraint.

Nomenclature

- σ = stress tensor
- p, s = hydrostatic and deviator parts of the stress tensor
- H = enthalpy
- Q_{rad} = heat flux by radiation
- $Q_{\text{closed}}, Q_{\text{open}}$ = heat flux at the contact interface (closed- and open-gap models)
- $h_{\text{closed}}, h_{\text{open}}$ = heat transfer coefficients (closed- and open-gap models)

$T_{\text{mould}}, T_{\text{cast}}, T_{\text{env}}$ = mold, casting, and environment temperatures
 t_n = contact pressure
 g_n = normal gap (open air gap)

References

- [1] Brezzi, F., and Fortin, M., 1991, *Mixed and Hybrid Finite Element Methods*, Springer, New York.
- [2] Agelet de Saracibar, C., Chiumenti, M., Valverde, Q., and Cervera, M., 2006, "On the Orthogonal Subgrid Scale Pressure Stabilization of Finite Deformation J2 Plasticity," *Comput. Methods Appl. Mech. Eng.*, **195**, pp. 1224–1251.
- [3] Cervera, M., Chiumenti, M., Valverde, Q., and Agelet de Saracibar, C., 2003, "Mixed Linear/Linear Simplicial Elements for Incompressible Elasticity and Plasticity," *Comput. Methods Appl. Mech. Eng.*, **192**, pp. 5249–5263.
- [4] Chiumenti, M., Valverde, Q., Agelet de Saracibar, C., and Cervera, C., 2002, "A Stabilized Formulation for Elasticity Using Linear Displacement and Pressure Interpolations," *Comput. Methods Appl. Mech. Eng.*, **191**, pp. 5253–5264.
- [5] Chiumenti, M., Valverde, Q., Agelet de Saracibar, C., and Cervera, C., 2004, "A Stabilized Formulation for Incompressible Plasticity Using Linear Triangles and Tetrahedral," *Int. J. Plast.*, **20**, pp. 1487–1504.
- [6] Codina, R., 2000, "Stabilization of Incompressibility and Convection Through Orthogonal Sub-Scales in Finite Element Methods," *Comput. Methods Appl. Mech. Eng.*, **190**, pp. 1579–1599.
- [7] Cervera, M., Agelet de Saracibar, C., and Chiumenti, M., 1999, "Thermo-Mechanical Analysis of Industrial Solidification Processes," *Int. J. Numer. Methods Eng.*, **46**, pp. 1575–1591.
- [8] Chiumenti, M., Agelet de Saracibar, C., and Cervera, M., 1999, "Constitutive Modelling and Numerical Analysis of Thermomechanical Phase-Change Systems," CIMNE, Monograph M48, Barcelona.
- [9] Hallam, C. P., Griffiths, W. D., and Butler, N. D., 2000, "Modelling of the Interfacial Heat Transfer Between an Al-Si Alloy Casting and a Coated Die Steel," *Proceedings of IX International Conference on Modelling of Casting, Welding and Advanced Solidification Processes*.
- [10] Ransing, R. S., and Lewis, R. W., 1998, "Thermo-Elasto-Visco-Plastic Analysis for Determining Air Gap and Interfacial Heat Transfer Coupled With the Lewis-Ransing Correlation for Optimal Feeding Design," *Proceedings of VIII International Conference on Modelling of Casting, Welding and Advanced Solidification Processes*, San Diego, CA.
- [11] Wriggers, P., 2002, *Computational Contact Mechanics*, Wiley, New York.
- [12] Wriggers, P., and Zavarise, G., 1993, "Thermomechanical Contact: A Rigorous but Simple Numerical Approach," *Comput. Struct.*, **46**, pp. 47–53.
- [13] Laursen, T. A., and Simo, J. C., 1993, "A Continuum-Based Finite Element Formulation for the Implicit Solution of Multibody, Large Deformation Frictional Contact Problems," *Int. J. Numer. Methods Eng.*, **36**, pp. 3451–3485.
- [14] Agelet de Saracibar, C., 1998, "Numerical Analysis of Coupled Thermo-Mechanical Frictional Contact Problems. Computational Model and Applications," *Arch. Comput. Methods Eng.*, **5**, pp. 243–301.
- [15] Ju, J. W., and Taylor, R. L., 1998, "A Perturbed Lagrange Formulation for the Finite Element Solution of Non-Linear Frictional Contact Problems," *Journal of Theoretical and Applied Mechanics*, **7**, pp. 1–14.
- [16] Jaouen, O., and Bellet, M., 1998, "A Numerical Mechanical Coupling Algorithm for Deformable Bodies: Application to Part/Mold Interaction in Casting Process," *Proceedings of VIII International Conference on Modelling of Casting, Welding and Advanced Solidification Processes*, San Diego, CA.
- [17] Nour-Omid, B., and Wriggers, P., 1987, "A Note on the Optimum Choice for Penalty Parameter," *Commun. Appl. Numer. Methods*, **3**, pp. 581–585.
- [18] VULCAN, Software for Simulation of Casting Processes, QUANTECH-ATZ, <http://www.quantech.es/QuantechATZ/Vulcan.html>
- [19] Nishida, Y., Droste, W., and Engler, S., 1986, "The Air-Gap Formation Process at the Casting-Mould Interface and the Heat Transfer Mechanism Through the Gap," *Metall. Trans. B*, **17B**, pp. 833–844.
- [20] Agelet de Saracibar, C., Cervera, M., and Chiumenti, M., 2001, "On the Constitutive Modelling of Coupled Thermomechanical Phase Change Problems," *Int. J. Plast.*, **17**, pp. 1565–1622.
- [21] Agelet de Saracibar, C., Cervera, M., and Chiumenti, M., 1999, "On the Formulation of Coupled Thermoplastic Problems With Phase-Change," *Int. J. Plast.*, **15**, pp. 1–34.